

# ***Evaporative Metal Bonding of APMT to Nickel Superalloys***

**University Turbine Systems Research (UTSR) Workshop  
Purdue University  
November 4, 2015**

**John P. Hurley and Matthew N. Cavalli  
University of North Dakota**



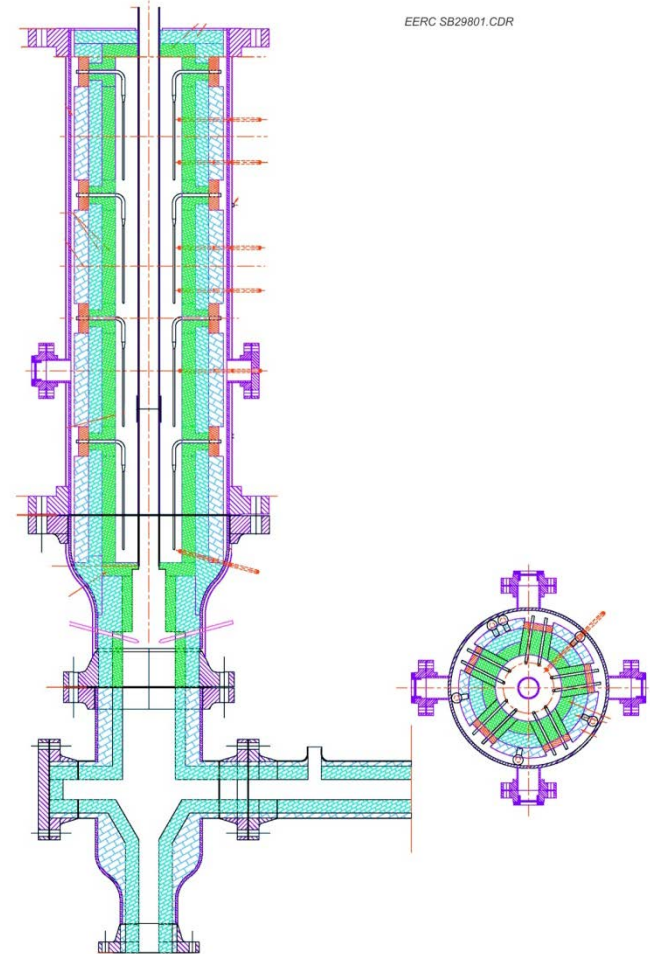
**Energy & Environmental Research Center (EERC)**

# Project Overview

- The University of North Dakota (UND) Energy & Environmental Research Center (EERC) and Department of Mechanical Engineering are working with Siemens Energy to test a new method for joining high-temperature alloys for use in advanced high-hydrogen-gas-burning turbines.
- Developed models for designing clamping fixtures and zinc diffusion.
- Thin plates of oxidation- and spallation-resistant Kanthal APMT™ have been bonded to high-strength CM247LC and Rene® 80 using evaporative metal (EM) bonding.
- Bonded parts, with and without thermal barrier coatings (TBCs), will be tested for oxidation, corrosion, and spallation resistance at Siemens Energy.
- Gasifier sampling to determine appropriate corrosion conditions.

# Characterization of Combusted Syngas Contaminants

- Information to be used in designing later corrosion testing – contaminants will not be similar to gasifier fly ash.
- Collection of microcontaminants in combusted syngas created in two pilot-scale gasifiers.
- Analysis of captured microcontaminants by SEM.





# EERC Pilot-Scale Gasifiers

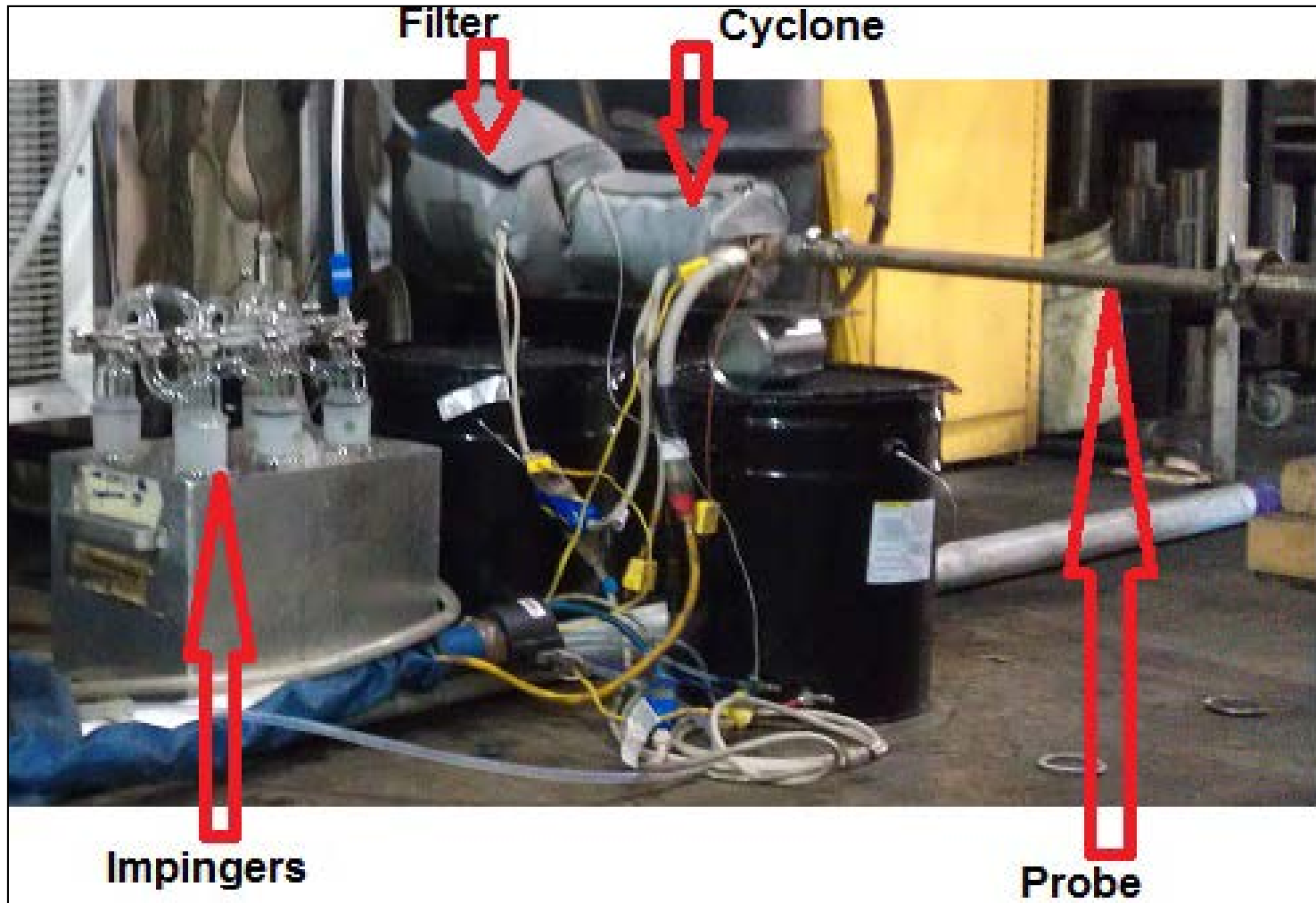


Entrained-Flow Gasifier (EFG)  
1800°C, 300 psi

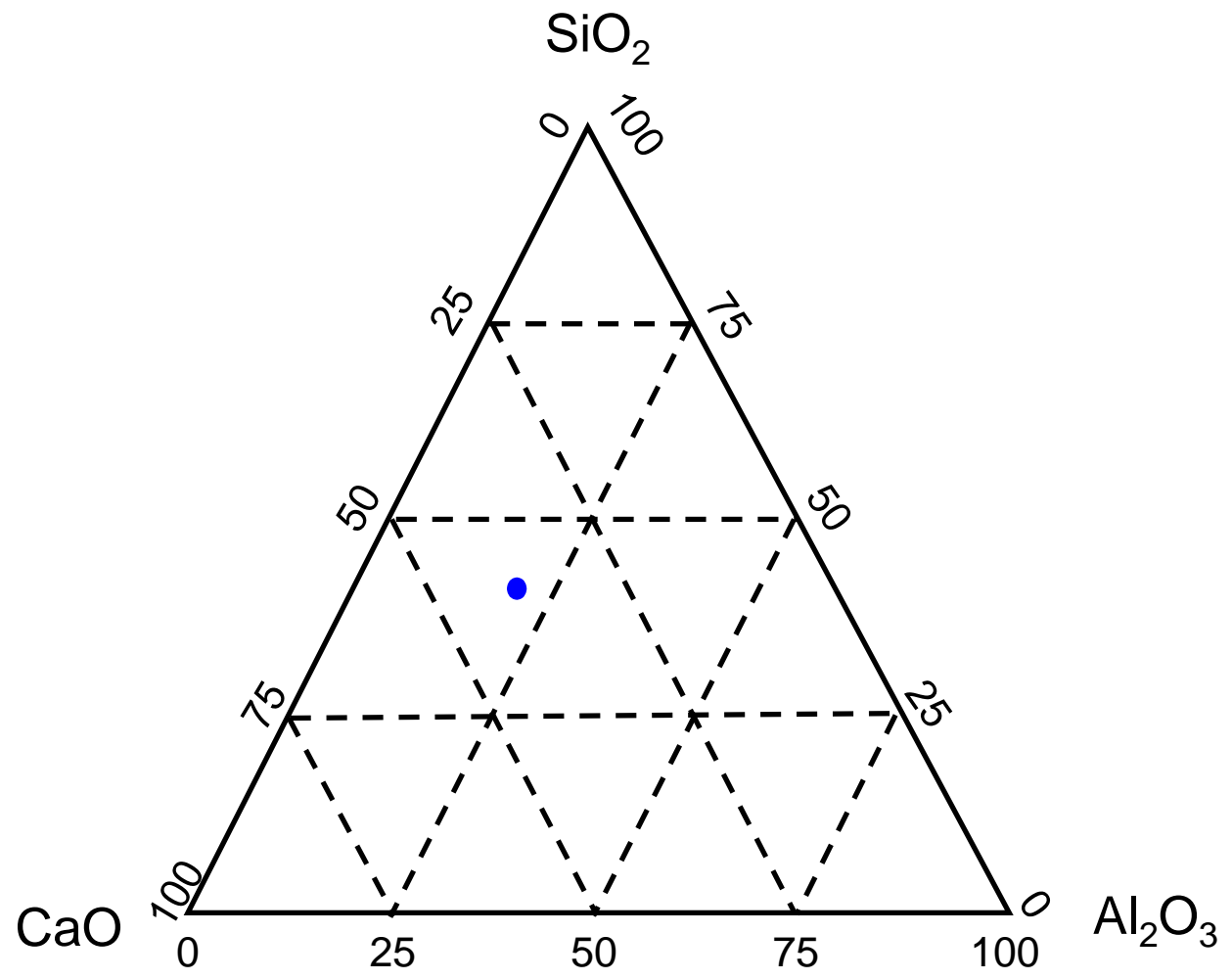


Fluid-Bed Gasifier (FBG)  
800°C, 600 psi

# Method 29 Sampling System

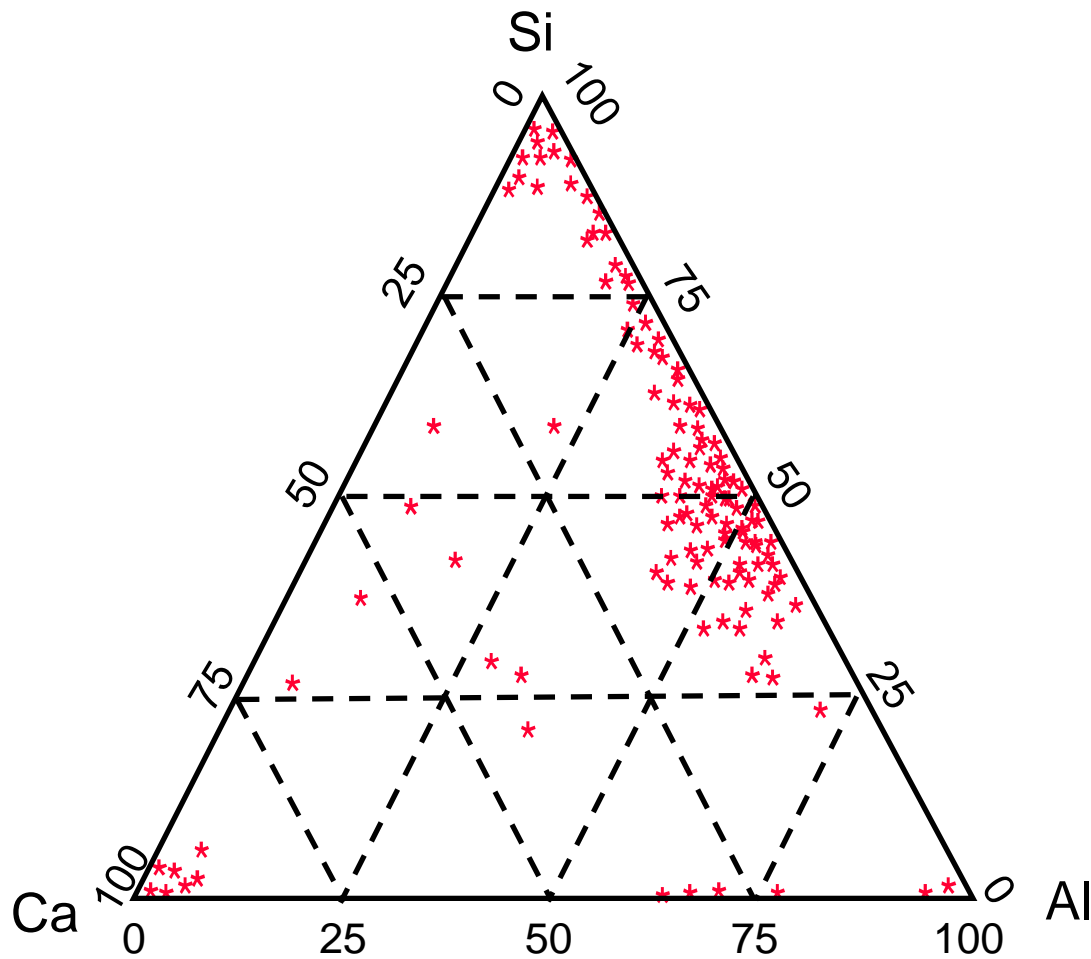


# Eagle Butte Coal Ash Composition



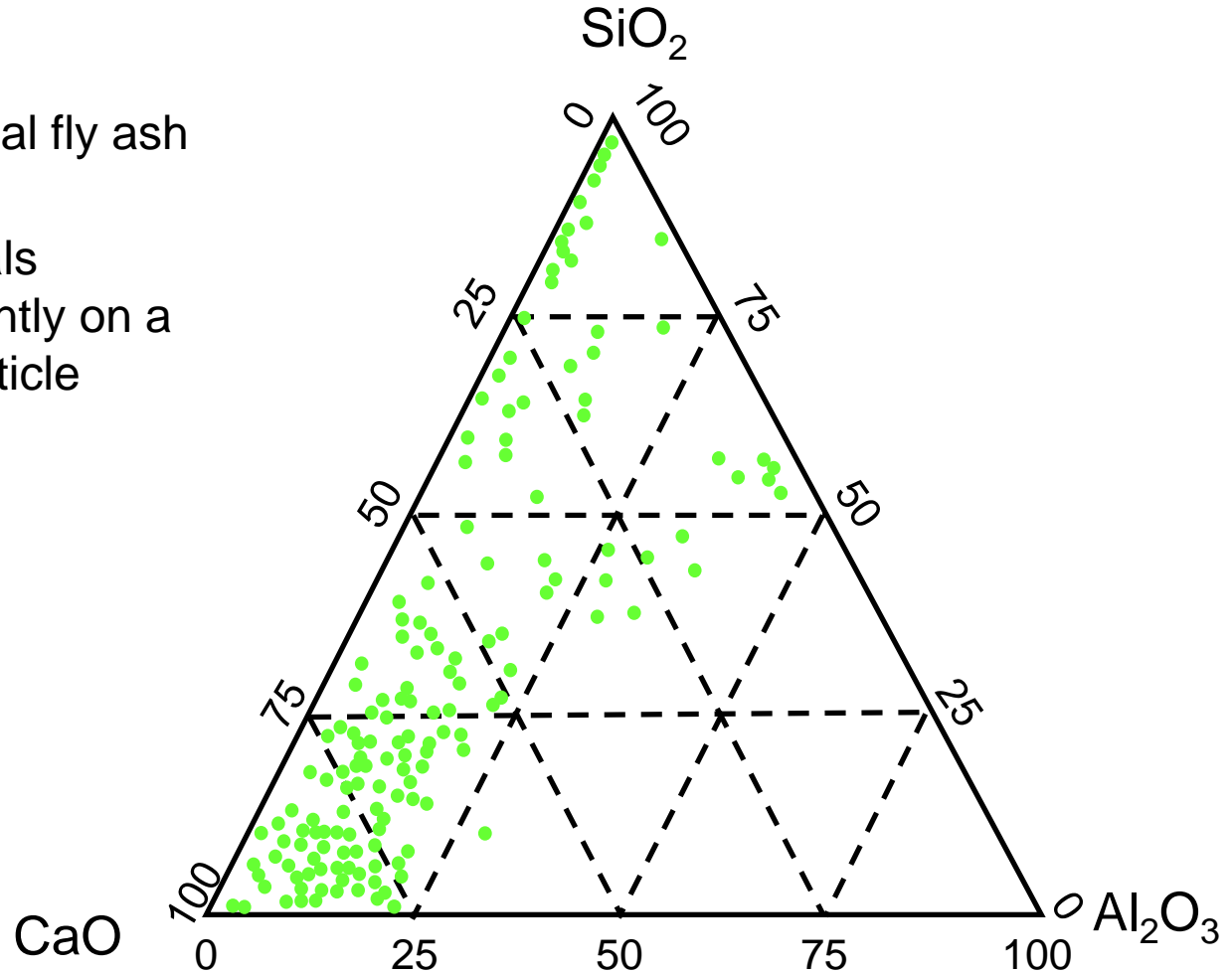


# Eagle Butte Coal Mineral Compositions



# Advanced Technique Analysis for Eagle Butte Fly Ash

- Plot of individual fly ash minerals.
- Fly ash minerals behave differently on a particle-by-particle basis.





# Results of FBG Particulate Analyses

- In the quenched syngas, the particulates are predominantly 0.1–0.5  $\mu\text{m}$  in diameter.
- We were not able to get good energy-dispersive x-ray analyses of the small predominant particles.
- XPS shows that the average composition of the syngas particles is very close to that of the polycarbonate filter and is most likely carbonaceous soot.
- In the combusted syngas, the carbonaceous particles are more spherical than in the syngas and slightly larger, typically 0.2–2  $\mu\text{m}$ .
- The combusted particles show more O, N, and S than the noncombusted particles.
- Ion etching shows that the increased O, N, and S were confined to the surface of the particles.

# Results of EFG Particulate Analyses

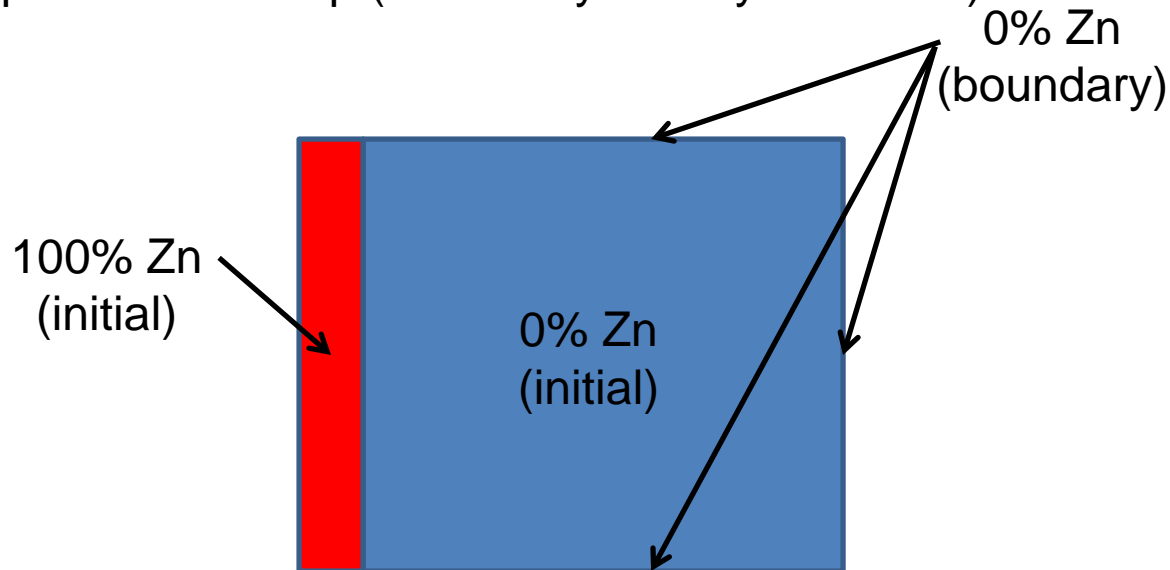
- No submicron particulates were seen on the syngas filter either because the filter had softened or there is just less soot formed due to the lower tar formation in an EFG.
- Flakes of iron oxide were collected from the syngas that came from system surfaces. They contained some C, Na, Cl, S, and Zn.
- Combusted syngas contained 0.1 to 0.3 micron soot particles.
- Some soot is collected even when burning only natural gas, but particles are smaller and fewer than when burning syngas.

# Diffusion Modeling

$$\frac{\partial C}{\partial t} = D \left[ \frac{\partial^2 C}{\partial x^2} + \frac{\partial^2 C}{\partial y^2} + \frac{\partial^2 C}{\partial z^2} \right]$$

3-D Diffusion with Constant Diffusivity

No analytical solution exists for the combination of initial and boundary conditions present in the experimental setup (midline symmetry assumed):

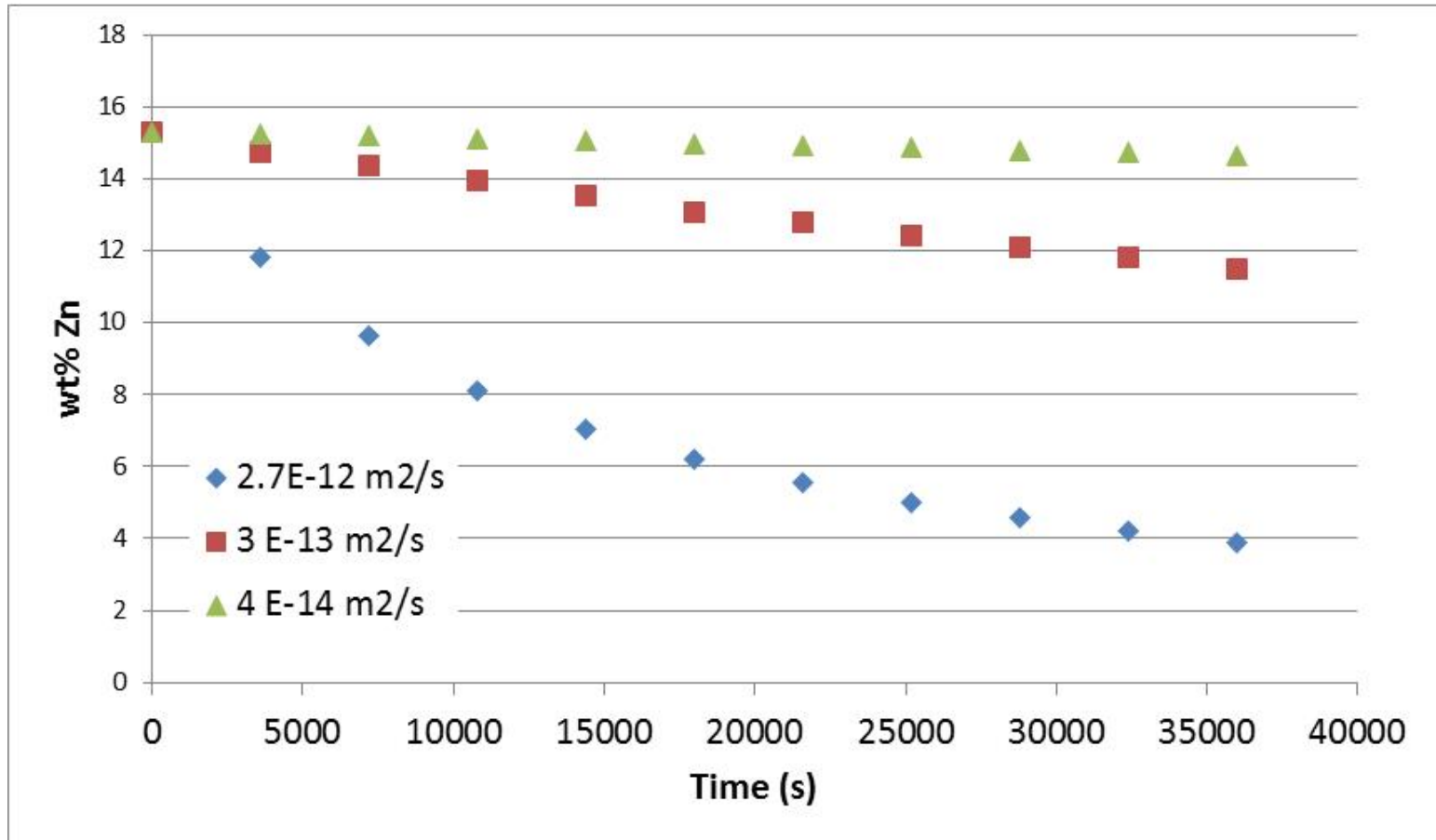


# Diffusion Modeling

- A finite difference algorithm was implemented within MATLAB to solve the diffusion equation.
- The 'hopscotch' iterative solver was implemented to improve accuracy and computational efficiency.
- Algorithm assumes initial midline concentration of Zn, assumes constant diffusivity, uses a rectangular geometry and allows for different mesh size in each direction (x, y, z).

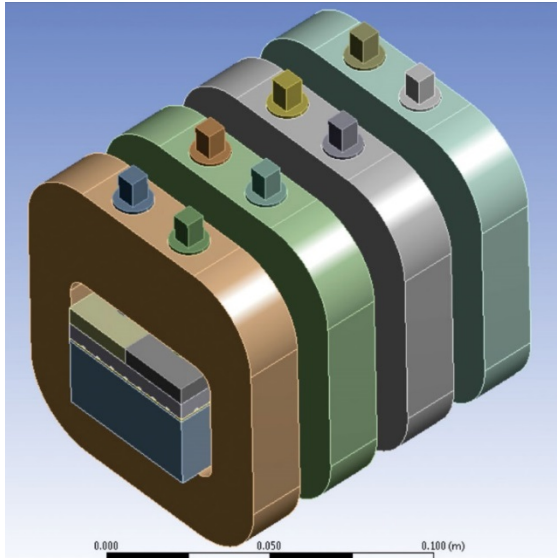


# Diffusion Modeling

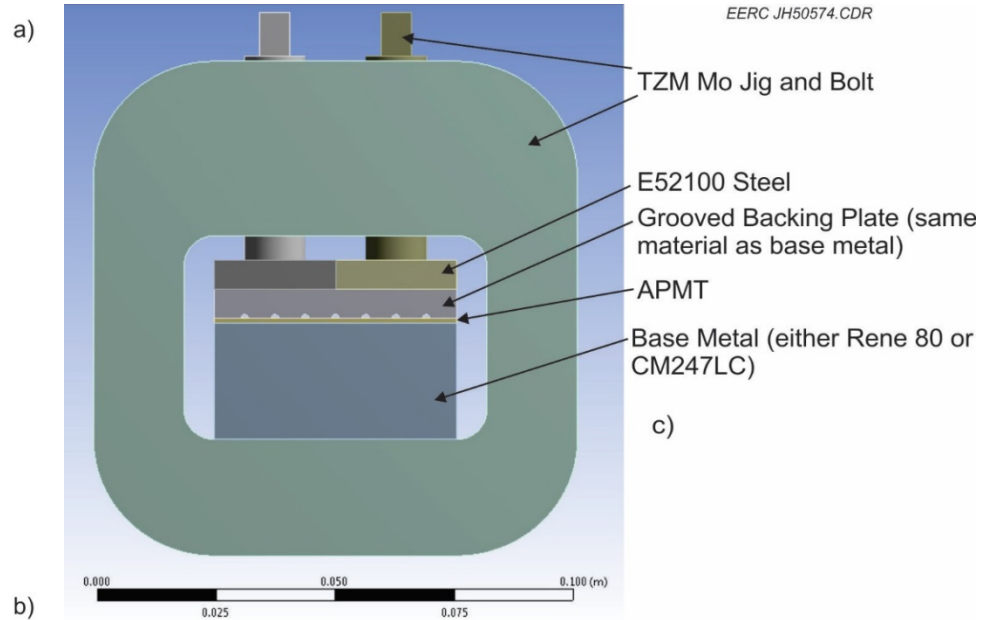
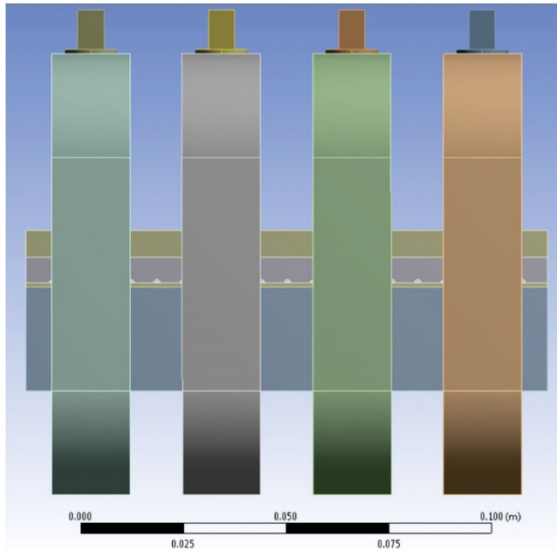


- ~15 wt% initial centerline composition for model
- D for Zn in APMT ~2.7 E-12 m<sup>2</sup>/s
- D for Zn in Rene 80/CM 247 ~4 E-14 m<sup>2</sup>/s

# Jig Assembly for Fabrication of Samples

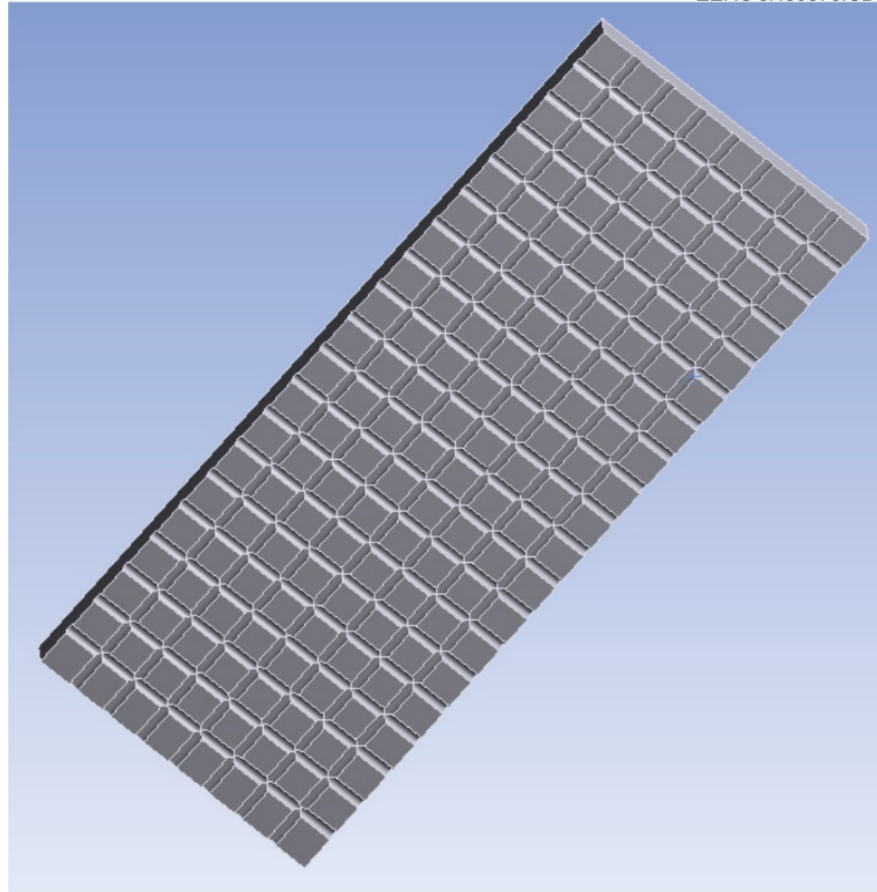


EERC JH50573.CDR

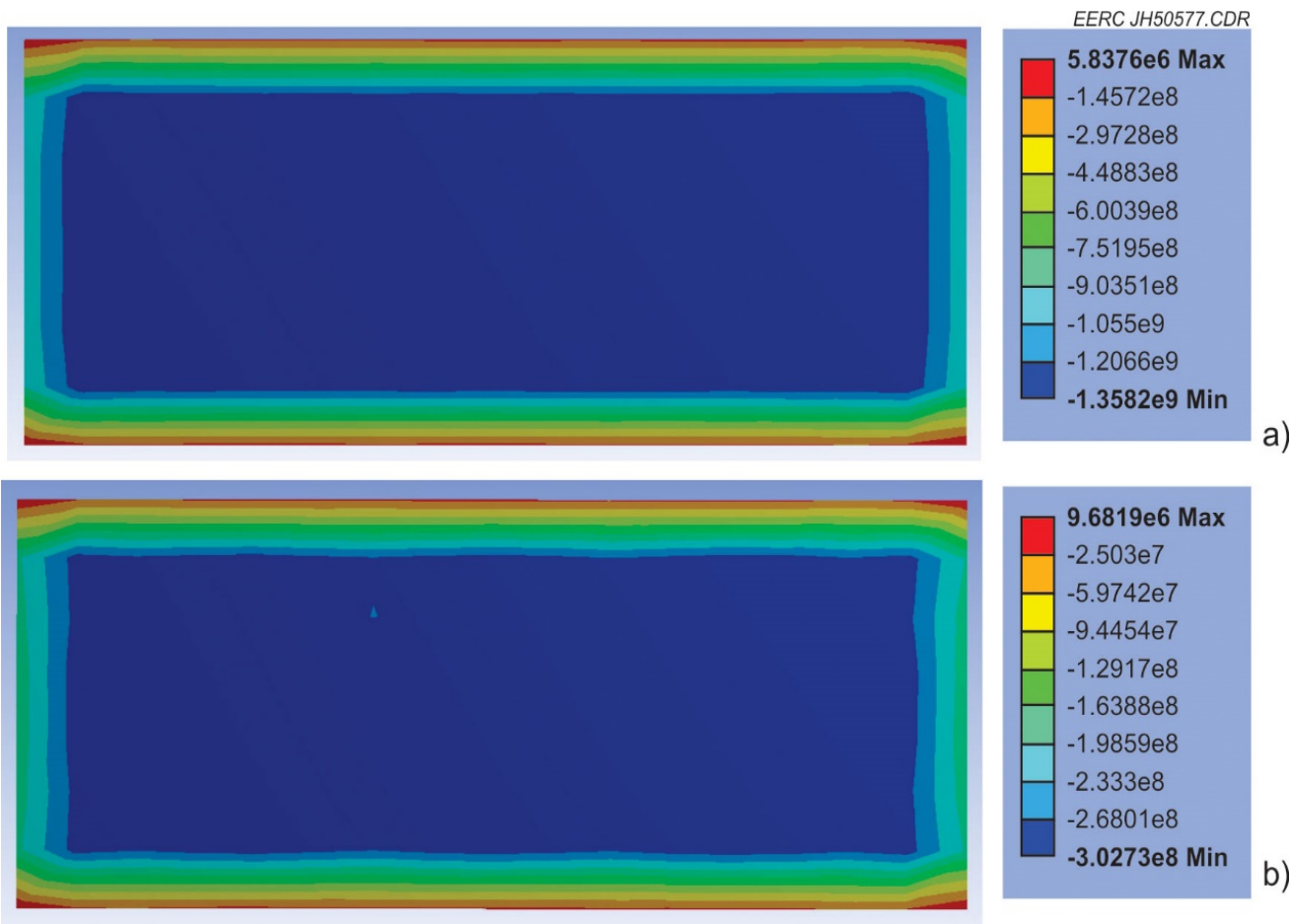


# Grooved Backing Plate

EERC JH50575.CDR

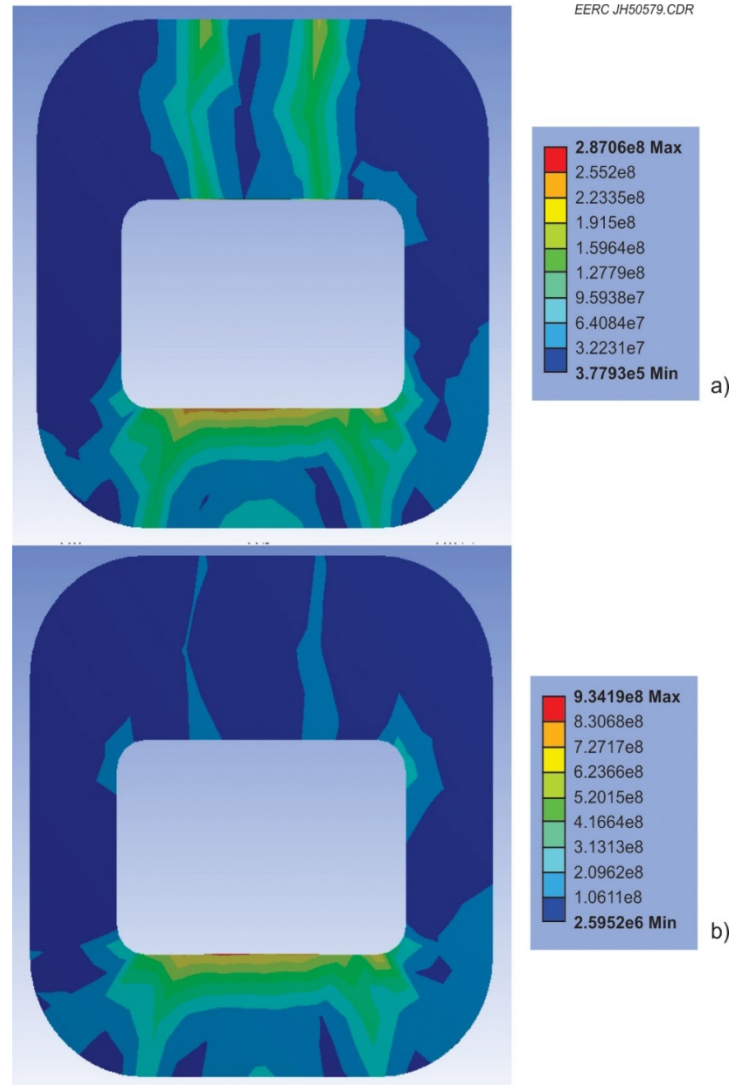


# Normal Stresses in the Plane for the APMT for CM247LC and Rene 80 at 1200°C

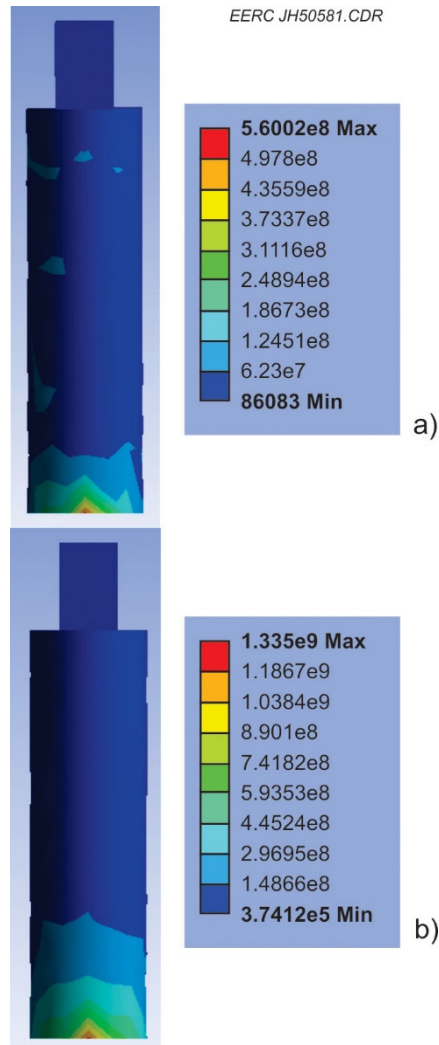




# TZM Mo Jig Equivalent Stresses for CM247LC and Rene 80 at 1200°C



# Base Metal–TZM Mo Jig Normal Stresses for CM247LC and Rene 80 at 1200°C



# Assembled Jib in Preparation to Bond the APMT Plate to the Superalloy Block



# Alloy Compositions

## Composition of Kanthal APMT, wt% – Dispersion-Strengthened

	Cr	Al	Mo	Mn	Si	Fe
APMT	22	5	3	0.4	0.7	Balance

## Composition of CM247 LC, wt% – Gamma Prime-Strengthened

	Fe	Ni	Cr	Al	Ti	Co	Mo	Ta	W	Nb	Hf	Mn	Si
CM247LC	–	Balance	8.1	5.6	0.7	9.5	0.5	3.2	9.5	0.1	1.4	–	–

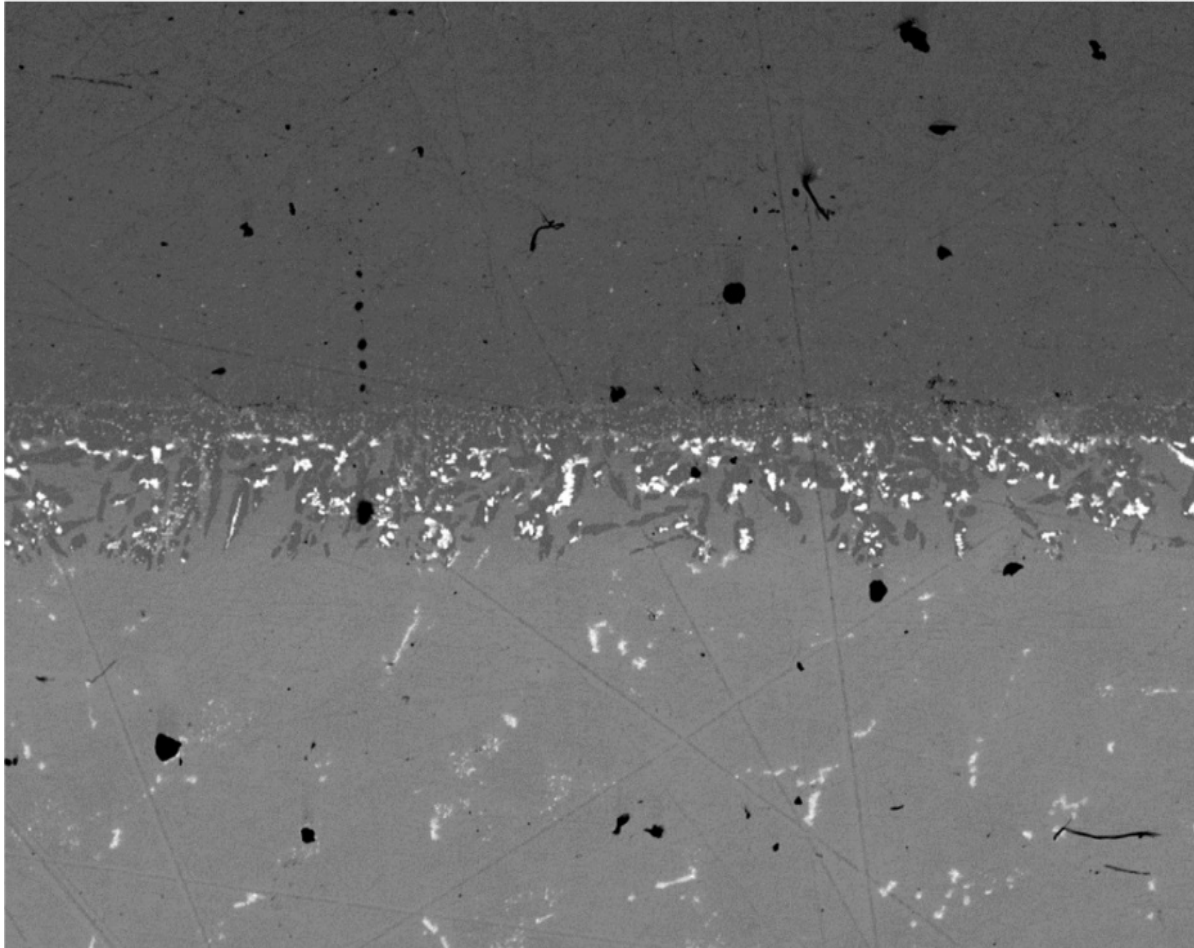
## Composition of Rene 80, wt% – Gamma Prime-Strengthened

	Cr	C	Mo	W	Ti	Nb	Co	Al	B	Fe	Zr	Ni
Rene 80	14.2	0.16	4.0	4.1	5.1	0.03	9.4	3.0	0.02	0.10	0.04	Balance



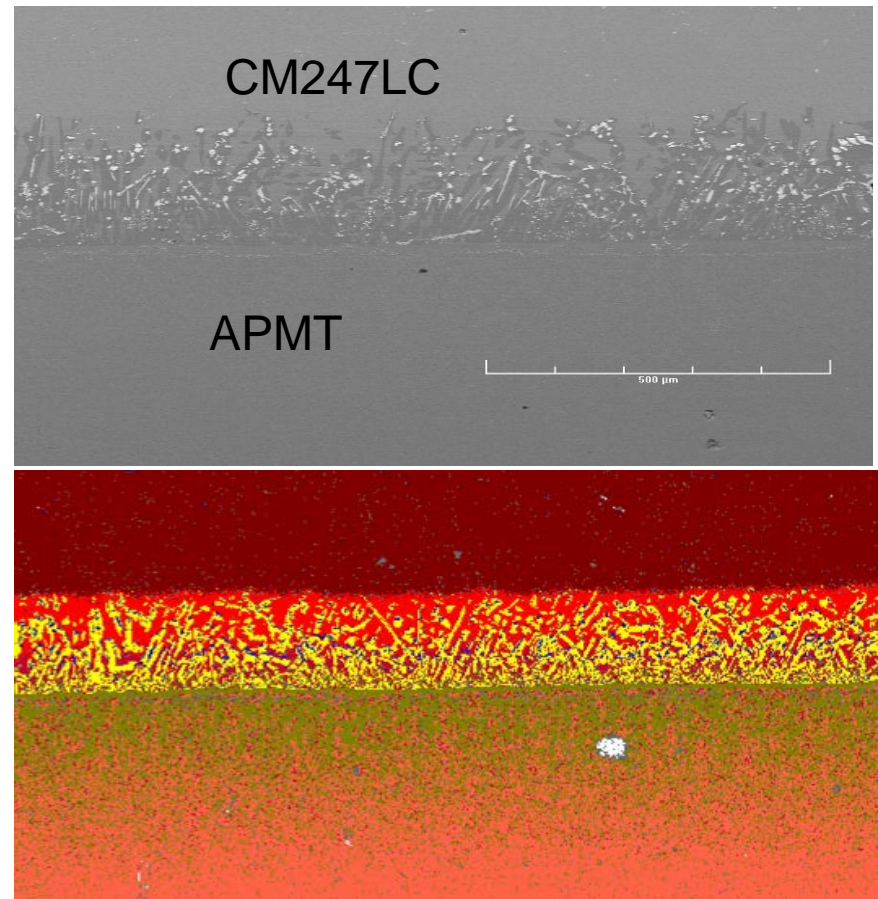
# Bond Line Between CM247LC (bottom) and APMT (top) at 100× Magnification

EERC JH51220.CDR

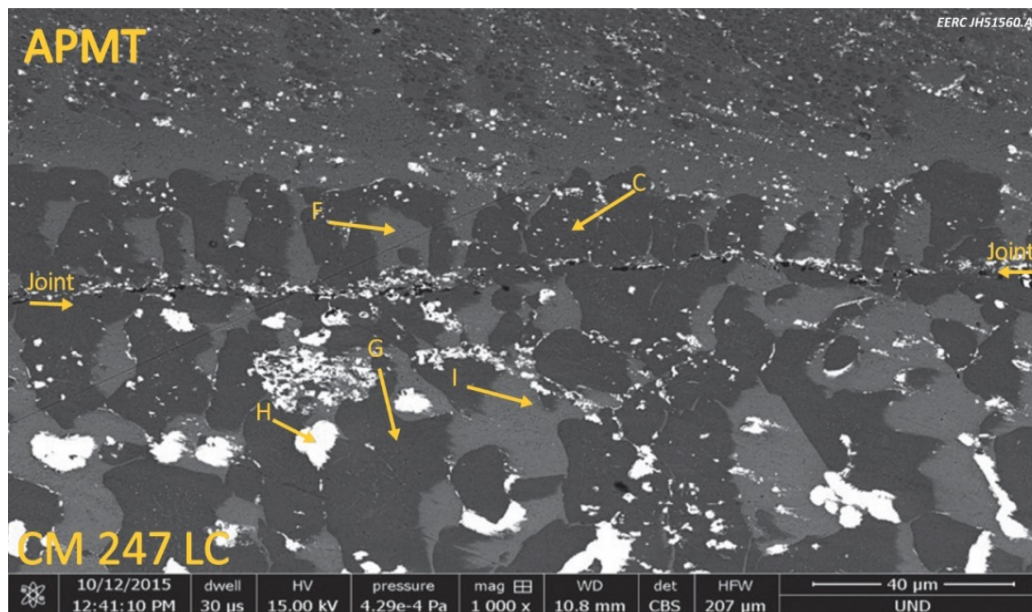


# Microstructure of EM Joints

- Scanning electron microscopy (SEM) photo (top) and x-ray map (bottom).
- Needle growth and interdiffusion to create a joint stronger than the APMT.
- Nickel diffuses up to 700  $\mu\text{m}$  into APMT.
- Iron diffuses 200  $\mu\text{m}$  into CM247LC.



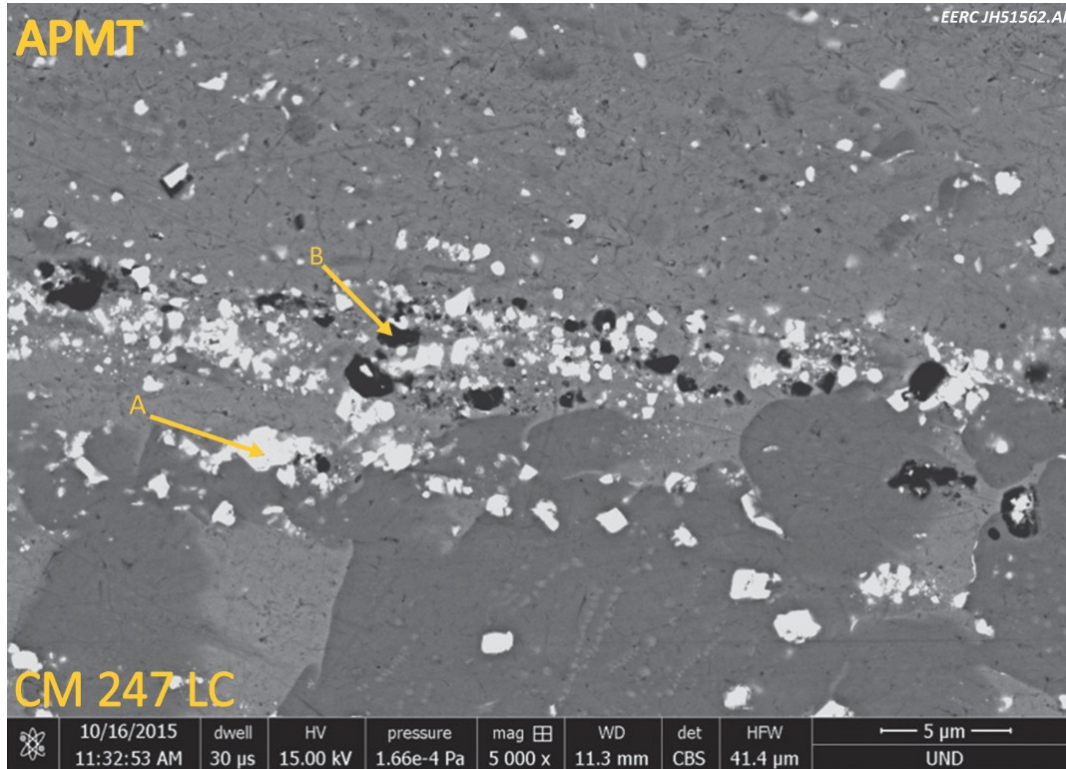
# Morphologies and Compositions in the APMT and the CM247LC Near the Bond Line at 1000x



	Element, wt%												
	Fe	Ni	Cr	O	Al	Mo	Hf	Ta	Ti	Mn	Zr	Co	W
C: Large, dark gray areas in APMT; from 0 to 30 μm into APMT	18.8	57.8	4.4	0.0	14.2	0.0	0.0	0.0	0.0	0.0	0.0	4.8	0.0
F: Large, light gray regions in APMT; present from 0 to 40 μm	41.2	29.1	13.7	0.0	2.6	1.1	1.0	1.5	0.0	0.0	0.0	5.3	4.5
G: Large, dark gray regions in CM247LC; present from 0 to 225 μm into CM247LC	15.1	58.7	2.8	0.0	12.8	0.0	1.8	3.1	0.4	0.3	0.0	5.0	0.0
H: Large, white regions in CM247LC; present from 40 to 260 μm	14.5	7.0	8.8	0.0	0.9	2.6	3.5	57.0	0.7	0.7	0.0	4.3	0.0
I: Large, light gray regions between precipitates in CM247LC	31.5	34.8	13.5	0.0	3.4	1.5	2.5	3.6	0.9	0.8	0.0	7.5	0.0



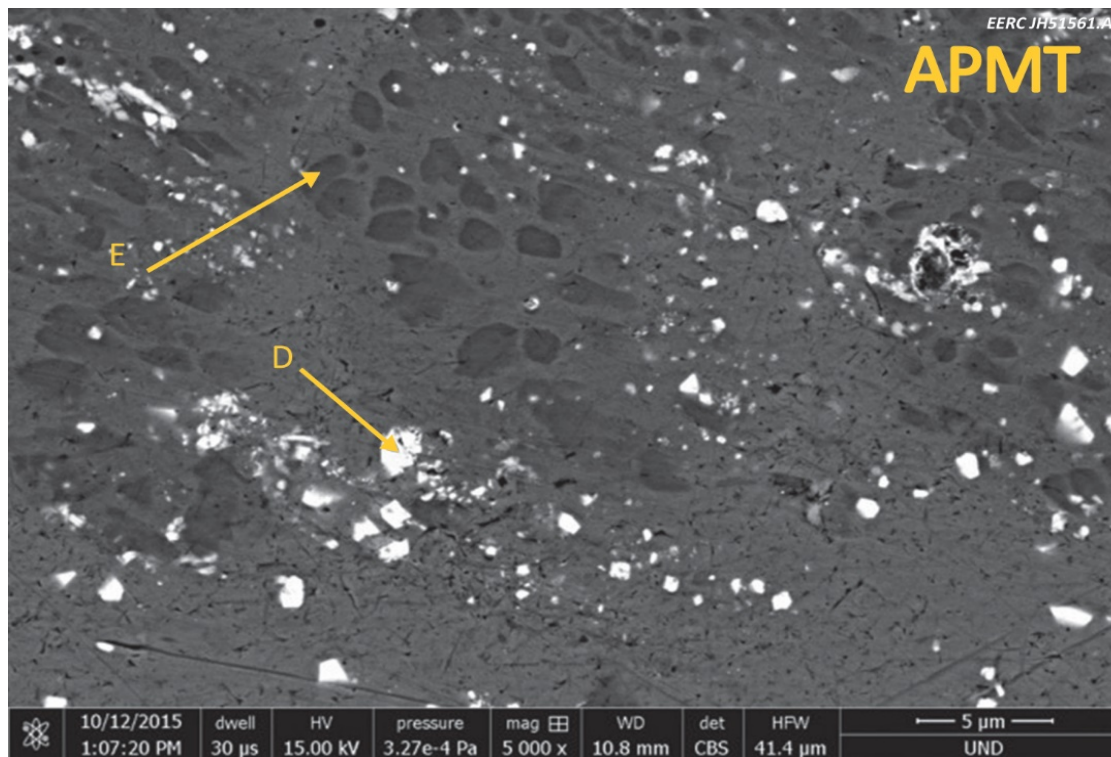
# Precipitates at the Bond Line of a CM247LC–APMT Joint at 5000×



	Element, wt%												
	Fe	Ni	Cr	O	Al	Mo	Hf	Ta	Ti	Mn	Zr	Co	W
A: Small white specks found along bond line	7.1	12.8	4.9	0.0	2.7	0.0	27.8	25.0	4.3	0.0	0.0	2.2	13.2
B: Black specks found along bond line	6.6	8.2	2.9	38.8	32.6	0.8	7.2	0.0	1.0	0.0	0.0	1.9	0.0



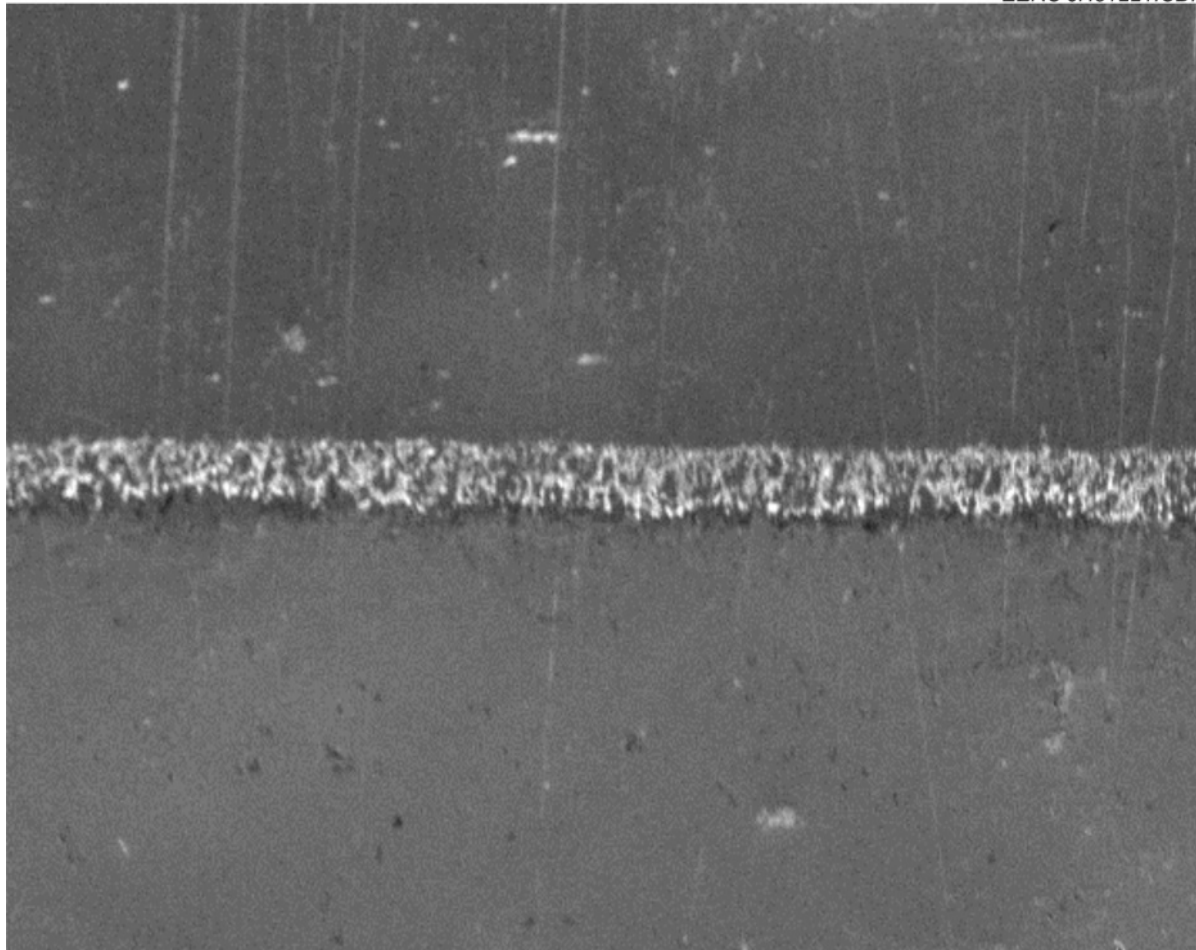
# Precipitates Within the APMT Near a CM247LC-APMT Joint at 5000x



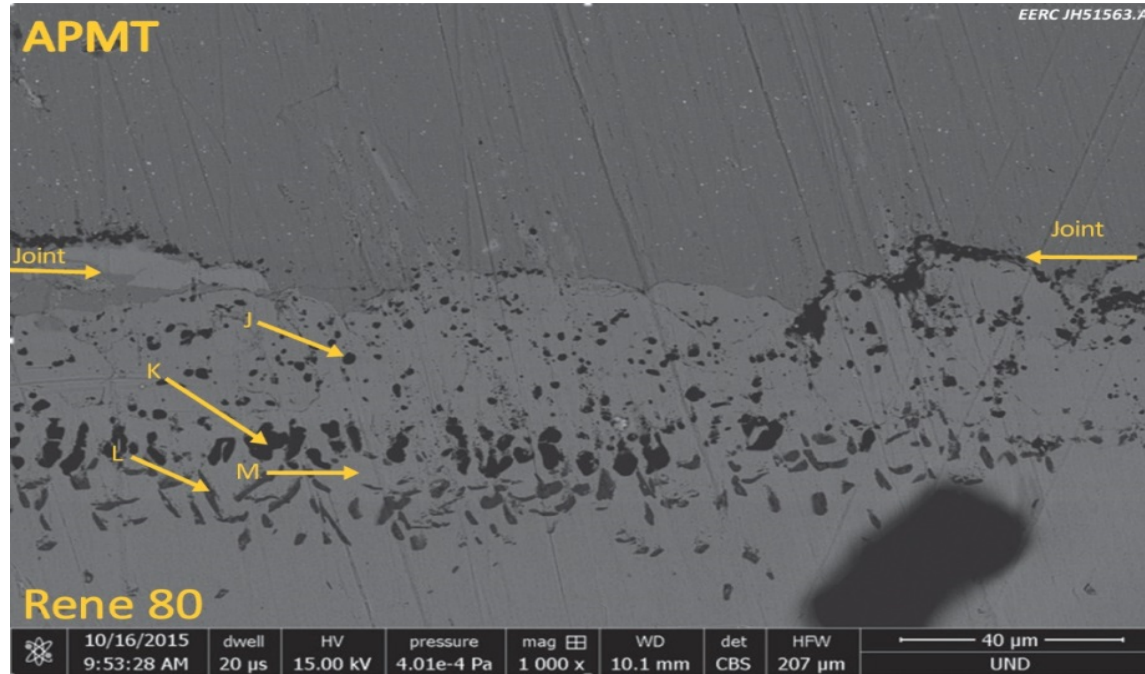
	Element, wt%												
	Fe	Ni	Cr	O	Al	Mo	Hf	Ta	Ti	Mn	Zr	Co	W
D: Small, white precipitates in APMT	8.3	3.3	3.0	0.0	0.6	0.2	23.8	42.8	14.5	0.1	2.7	0.7	0.0
E: Dark gray, small, and circular in APMT; present in APMT past 15 µm	22.7	49.5	6.5	0.0	13.4	0.3	1.0	2.8	0.2	0.2	0.0	3.4	0.0

# Bond Line Between Rene 80 (bottom) and APMT (top) at 100× Magnification

EERC JH51221.CDR



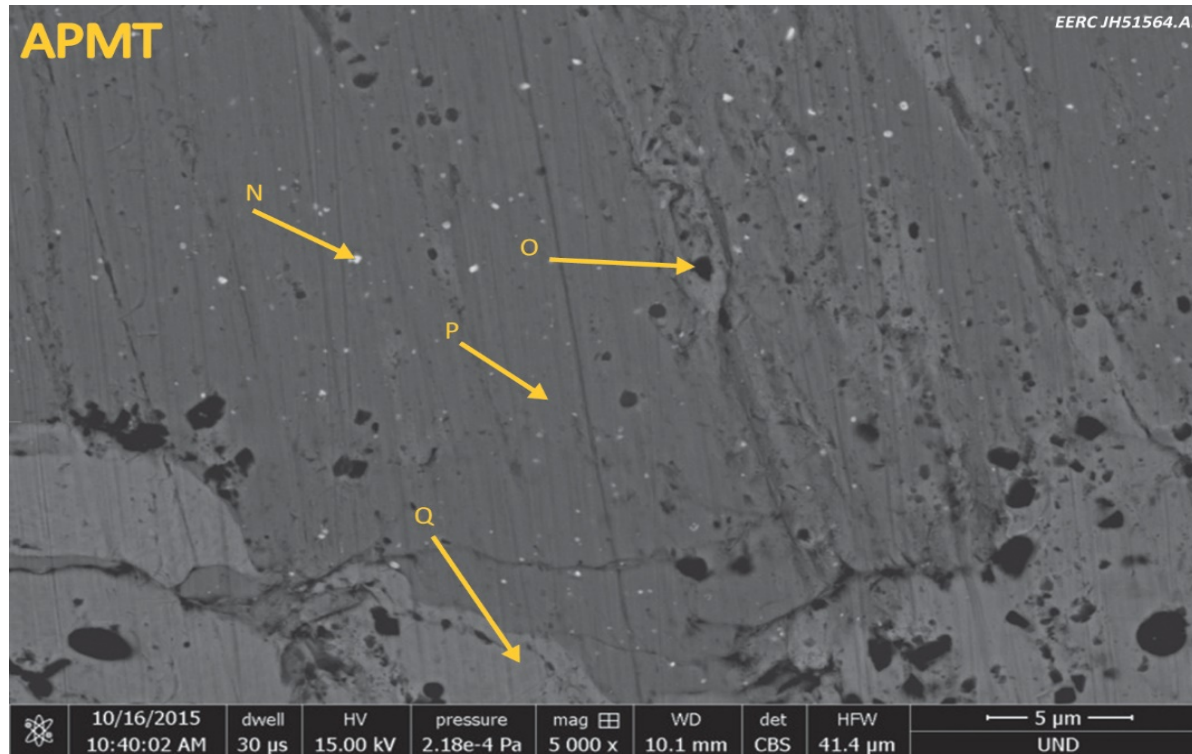
# Morphologies Near the Bond Line in an APMT–Rene 80 Joint at 1000×



	Element, wt%												
	Fe	Ni	Cr	O	C	Al	Mo	Ti	Co	W	Zr	Y	Si
J: Black and round precipitates in bond line; diffused up to 30 μm into base metal	2.7	12.3	4.0	37.9	6.1	33.6	0.0	0.8	2.6	0.0	0.0	0.0	0.0
K: Black precipitates in Rene 80; formed approx. 30–45 μm below bond line	0.0	2.0	0.7	47.0	3.1	47.2	0.0	0.0	0.0	0.0	0.0	0.0	0.0
L: Light gray, skinny, and long precipitates in Rene 80; formed approx. 45–60 μm below bond line	0.0	2.3	0.0	0.0	4.1	0.0	0.0	93.6	0.0	0.0	0.0	0.0	0.0
M: Gray regions in between other ppt.	3.7	64.0	8.9	0.0	3.8	3.4	3.2	3.4	9.6	0.0	0.0	0.0	0.0



# Precipitates in the APMT Near an APMT–Rene 80 Joint at 5000×



	Element, wt%												
	Fe	Ni	Cr	O	C	Al	Mo	Ti	Co	W	Zr	Y	Si
N: White specks in APMT	50.7	3.6	11.4	0.8	13.0	2.5	0.0	2.0	0.0	0.0	7.7	0.0	8.3
O: Black specks in APMT; from 0 to 30 μm	44.4	2.7	10.6	15.0	5.7	12.6	1.3	0.0	0.0	0.0	0.0	7.7	0.0
P: Gray region in APMT	68.3	3.8	15.5	0.0	5.2	4.4	2.8	0.0	0.0	0.0	0.0	0.0	0.0
Q: Gray region	69.7	4.8	15.3	0.5	3.0	3.9	2.6	0.0	0.0	0.0	0.0	0.0	0.2



# EM Bonding Initial Observations

- One bond for each superalloy was weak, likely due to oxidation during a month long period between sandblasting and bonding.
- Previous tests with CM247LC show bond is stronger than the APMT.
- The procedure allows all of the zinc to diffuse out down to the detection limit (0.1%) and evaporate from the surface.
- Most zinc diffusion occurs through the APMT.
- There is significant interdiffusion between the alloys, especially iron, nickel, tantalum, and hafnium, more with CM247LC than with Rene80.
- The interdiffusion causes precipitation of different phases near the bond line.

# Future Work

- Siemens Energy will perform precipitation hardening procedure on bonded superalloys.
- TBC will be applied to the APMT layer on a portion of the samples.
- They will then perform their standard oxidation, spallation resistance, and hot corrosion tests on the samples and compare to previous results for unbonded samples.
- EERC will perform hardness tests and SEM analyses on nonhardened and hardened crosssections.
- EERC will perform SEM analyses on oxidized and corroded samples. Will aluminum cross from the superalloy (source) to the APMT (sink)?

# Acknowledgments

- This material is based upon work supported by the U.S. Department of Energy (DOE) National Energy Technology Laboratory under Award No. DE-FE0007325.
- Siemens Energy Inc. for supplying superalloys, advice, and testing data.
- Josh Braband, Serges Nguelo, and Garrett Georgeson who are or were students in the UND Mechanical Engineering Department.

# Contact Information

## **Energy & Environmental Research Center**

University of North Dakota

15 North 23rd Street, Stop 9018

Grand Forks, ND 58202-9018

World Wide Web: **[www.undeerc.org](http://www.undeerc.org)**

Telephone No. (701) 777-5159

Fax No. (701) 777-5181

**John Hurley, Principal Materials Scientist**

**[jurley@undeerc.org](mailto:jurley@undeerc.org)**



## Disclaimer

This presentation was prepared as an account of work sponsored by an agency of the United States Government. Neither the United States Government, nor any agency thereof, nor any of their employees, makes any warranty, express or implied, or assumes any legal liability or responsibility for the accuracy, completeness, or usefulness of any information, apparatus, product, or process disclosed or represents that its use would not infringe privately owned rights. Reference herein to any specific commercial product, process, or service by trade name, trademark, manufacturer, or otherwise does not necessarily constitute or imply its endorsement, recommendation, or favoring by the United States Government or any agency thereof. The views and opinions of authors expressed herein do not necessarily state or reflect those of the United States Government or any agency thereof.